Switch-off mechanisms in GeAsTe Ovonic Threshold Switching Selector Device

Z. Hu[1], Z. Chai[2], W. Zhang[1], Jian Zhang[1]
[1]School of Engineering, Liverpool John Moores University, Liverpool L3 3AF, UK,
[2]Xi'an Jiaotong University, China

Abstract

Understanding the switching process in ovonic threshold switching (OTS) devices is an important research topic. Less attention has been paid to the fast switching-off process in the past, especially in modern nanoscale OTS devices. In this work, the OTS switching-off process in 1S1Rs operations are investigate. The underlying mechanisms can be explained by the dynamic resistance of OTS induced by the transition of defect clusters, and the impact of series resistance value on the switching off process is revealed. The defect cluster shrinking stage and rupture stage can be measured and characterized, respectively, which correspond to two distinct switch-off mechanisms. This research sheds new light on OTS switching mechanism and its impact on 1S1Rs operation.

1. Introduction

Selector device plays a key role in suppressing the sneak path currents in the crossbar arrays that utilize the emerging non-volatile memory devices [1, 2], such as the phase change memory (PCRAM) [3], the Redox based and oxide based resistive switching memory (ReRAM/OxRAM) [4]. The selector is required to have fast volatile switching characteristics and is connected in series with the non-volatile memory device. When the memory device is not selected, it is biased at a half of the operation voltage, at which the selector should have very low off-state current and can suppress the overall leakage current and avoid the sneak current path. When the memory device is selected at the operation voltage, the selector is at the ON state, and should allow a sufficiently high current to pass through so that the memory device can be programmed. A large on-off current ratio is an essential requirement for the selector, therefore [5]. Among the competing technologies, OTS selectors have achieved fast switching speed in the order of ns, high ON-state current density larger than 20MA/cm^2, high half-bias nonlinearity larger than 10^5, and excellent endurance >10^{12} cycles [6-8].

Despite the recent progress, further detailed electrical experimental evidence is needed to investigate the switching off process. Several new observations in GeAsTe OTS switching are investigated in this work, including the full OTS quasi-static switching-off process and two distinct mechanisms of OTS switch-off: the OTS switches off at zero total impedance of 1S1Rs when the Rs value is small, and it switches off at the minimum OTS current when Rs is large. It is found that the switching off process is associated with the defect cluster shrinking kinetics, which becomes Rs independent after the normalization. On the other hand, the rupture criteria of the defect cluster are dependent on Rs. Significant impact of Rs on the 1S1Rs operations and parameters are also identified.

2. Devices and Experiments

A 20nm amorphous GeAsTe chalcogenide film is deposited by room temperature physical vapor deposition (PVD) and passivated with a low-temperature BEOL process. The TiN/GeAsTe/TiN selector uses a pillar (TiN) bottom electrode that defines the device size down to 50 nm and integrates with a serial resistor Rs in the range of 1.8 kΩ to 400 kΩ in a 300 mm process flow, as shown in **Fig.1a**. The I-V characterization was carried out by using a Keithley 4200A semiconductor analyzer either with the SMU for DC sweep or with the embedded 4225-PMU ultrafast I-V module for voltage sweep. A typical DC I-V of the 1S1R measured by a triangular pulse is shown in **Fig. 1b,** from which the OTS-only I-V can be obtained by subtracting the voltage across the series Rs, $V_{OTS}=V_{1S1R}-I\cdot Rs$, since the linear I-V at ON-state is dominated by Rs, as illustrated in **Fig.2a**, in which V_{th} is the threshold voltage for off-to-on switching, V_{hold} is the voltage where the on-to-off switching occurs. Note that these values are different for 1S1R and OTS-only. The threshold current and holding current, on the other hand, are the same for 1S1R and OTS-only due to the series connection. The I-V curves with various Rs values are shown in **Fig. 2b** for the 1S1R, and in **Fig. 2c** for the extracted OTS-only, respectively. The larger Rs value leads to lower on-state and holding current, and larger threshold and holding voltage for the 1S1R. However, the OTS-only I-Vs in **Fig. 2c** follow a similar trajectory during the switching off process, demonstrating the validity of this extraction method, as the OTS in these devices have the same configuration and parameters.

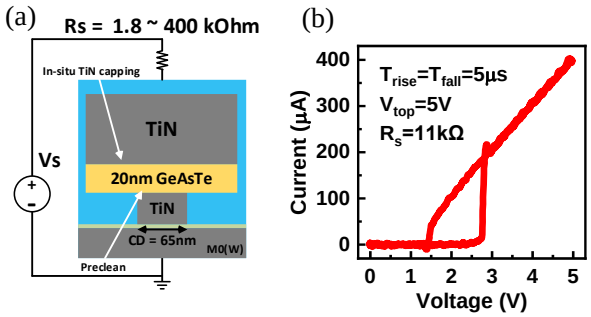

Fig. 1 Fig. 1 (a) Illustration of the OTS structure in series with a resistor Rs. (b) A typical I-V of 1S1Rs measured by a triangular pulse. Pulse conditions and Rs value are labelled. Device size (CD) is 65nm unless specified otherwise.

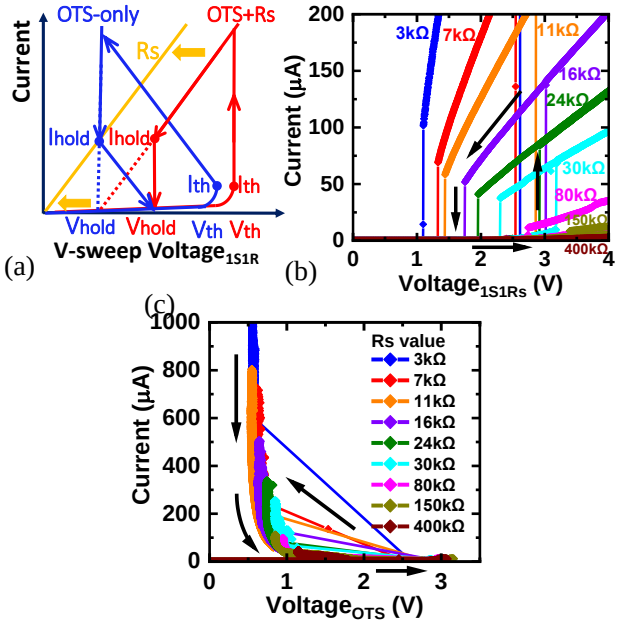

Fig. 2 (a) Illustration of OTS-only I-V extraction. (b) I-V during DC voltage sweep measured for 1S1Rs with 3kΩ ≤Rs ≤ 400kΩ, and (c) the extracted I-V for OTS-only.

3. Results and discussions

The switching process in OTS has been described by different models, including the earlier thermally induced instability model [9], the electronic injection induced space charge model [10], the impact ionization induced generation and recombination model [11], the thermally assisted charge hopping model [11], the field induced nucleation model [12], and more recently, the electric field induced local bond modification models [13-16]. In the latest models, the defects transition from the ground state to the excited state at a high field due to the local bonds modification and become delocalized, so that the defect clusters are formed which lead to the off-to-on switching, and vice-versa for the on-to-off switching at a low electric field where the local bonds configuration recovered, and defects return to ground state and become localized again.

Furthermore, the operation of 1S1Rs in which the selector is connected with a series resistor (Rs) were also investigated [17, 18], and it was suggested that the Rs plays an important role in the switching-on and switching-off process. For example, it was found that Rs defines the load line for the selector and hence its operation points and the holding current, so that the selector is either switching volatilely between the static off-state and on-state, or oscillating in the transitional negative-differential-resistance (NDR) state [19-22]. Despite these early efforts, detailed experimental evidence is still lacking for characterizing the fast and sharp switching off process in modern OTS devices. For example, it is not clear how the switching process and parameters in nanoscale OTS devices are affected by the series resistance and what are the corresponding OTS switching mechanisms, which should provide important information for understanding the operation and modelling of the 1S1R circuit.

A detailed inspection on the OTS-only I-V curves can reveal more significant differences in the switching process. For smaller Rs values in the range below 30 kΩ, the I-V curves largely follow the same trajectory, as shown in Fig. 2c, agreeing with previous results [23]. However, as shown in Fig.3a, for larger Rs values at and above 80 kΩ, a significant non-linear ON state (NL-ON) region is observed, before the OTS switches to the OFF state, which deviates from the linear ON state that is defined by the Rs value. The origin of this NL-ON region needs to be investigated, as it could cause large errors if the Rs values in the 1S1Rs structure are read out from the current measured within this region. To rule out the possible contribution to this non-linear deviation by the test methods and speed, the results of DC voltage sweep, DC current sweep, and pulse voltage sweep with Rs = 80 kΩ are compared in Fig. 3b and Fig. 3c, respectively. The NL-ON region is observed and overlaps in all three cases, and similar results are also observed at other Rs values larger than 80kΩ. This confirms that the NL-ON is not caused by the test methods or speed used in our measurements, hence the instrument settings and the RC effects in the probe and cable connections are not responsible for the occurrence of NL-ON.

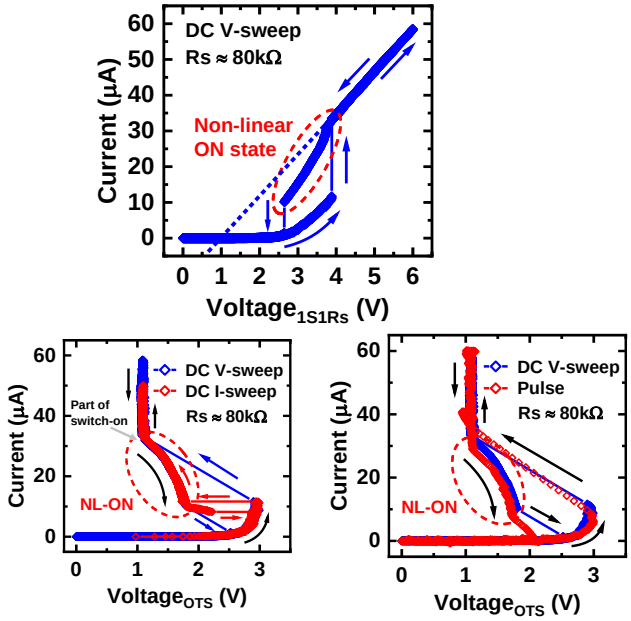

Fig. 3 (a) A significant non-linear ON state (NL-ON) region is observed before the OTS switches to OFF state with Rs≈80 kΩ. (b) Both DC V-sweep and I-sweep show NL-ON that overlap with each other during switch-off, and also overlap with a part of switch-on of DC V-sweep. (c) Good agreement is observed in DC and pulse V-sweep, supports that NL-ON is not caused by the measurement speed in our setup.

It is well known that the OTS device exhibits a negative differential resistance region during the switching process, as evident in **Fig. 3**. For the off-to-on voltage sweeps, the OTS current increases abruptly at V_{th}, and reaches the ON state at near the top end of, and in some cases just within the NL-ON region. For the on-to-off voltage sweeps, the OTS goes through the NL-ON region as the current reduces, until it reaches the holding point where the device switches off abruptly. The negative differential resistance in this large NL-ON region can be clearly seen, in which $dV_{OTS}/dI_{OTS} < 0$.

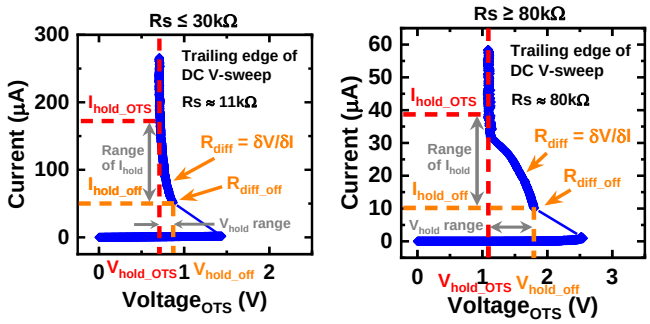

Fig. 4 Definition of Vhold_OTS, Ihold_OTS, Vhold_off and Ihold_off for OTS-only (a) when Rs≤30kΩ, and (b) when Rs≥80kΩ.

In contrast, when Rs is smaller than 80 kΩ, a much subtler NL-ON region is observed, as shown in Fig. 4a for Rs =11 kΩ, where the subtler NL-ON only slightly deviates from the linear ON region. This confirms that this significant difference in the OTS switching off process can only be caused by the difference in Rs values. A part of the UP traces when reaching the ON state also falls within the NL-ON region and overlap with the DOWN traces in Fig.3, suggests that the NL-ON is a common feature for both the switch-on and -off processes.

As described in the latest models, the defects return from the delocalized excited state to the localized ground state during the switching-off process, so that the conductivity of OTS decreases. From the above analysis, this process starts whilst the OTS is still at ON-state and its negative differential resistance increases when the electric field is getting smaller. To characterize the NL-ON region in the switching-off process, $R_{diff\_OTS} = \delta V_{OTS}/\delta I_{OTS}$ is defined as the dynamic differential resistance of OTS-only, as shown in Figs. 4a&b, with smaller and larger Rs values, respectively. R_{diff_OTS} is negligible in the linear ON state, where the linear I-V is dominated by Rs. The I-V curves enter the NL-ON at (I_{hold_OTS}, V_{hold_OTS}), where the increase of $|R_{diff\_OTS}|$ is no longer negligible in comparison to Rs, due to the defect clusters shrinking with the decreasing current [14]. The OTS switches off at (I_{hold_off}, V_{hold_off}) when the defect clusters rupture, and this is the OTS holding point commonly used for 1S1R [13, 14, 24], where $R_{diff\_OTS} = R_{diff\_off}$. The switching-off process is clearly different for Rs≤30 kΩ and Rs≥80 kΩ as Fig.4 shows it is controlled by different mechanisms.

The impact of Rs on the boundary condition of the NL-ON region, i.e., (I_{hold_OTS}, V_{hold_OTS}) and (I_{hold_off}, V_{hold_off}), is further examined. **Fig. 5** shows that I_{hold_OTS} decreases inversely with Rs, agreeing with previous works that follows a linear line in the log-log scale [20]. At the onset point of the NL-ON region, the total differential resistance is dominated by Rs, so the inverse relation between I_{hold_OTS} and Rs is as expected, since the OTS operates with Rs as the load, and (I_{hold_OTS}, V_{hold_OTS}) is the on-set of defect cluster shrinking in the OTS when the differential resistance of OTS starts to become negative. I_{hold_off} also decreases inversely when Rs is small (Rs ≤ 30kΩ), as expected. But for larger Rs values (Rs ≥ 80kΩ), I_{hold_off} no longer decreases with Rs and remains at a constant minimum value just below 10 μA. This provides clear evidence that there are two distinct switching-off mechanisms, associated with small and large Rs values, respectively. As shown in **Fig.5b**, for the smaller Rs, OTS switches off when $|R_{diff\_OTS}|$ reaches Rs (≤30 kΩ), where the total impedance of the 1S1Rs circuit, $Rs+R_{diff\_OTS}$, becomes 0. For larger Rs, the maximum value of $|R_{diff\_OTS}|$, $|R_{diff\_max}|$, becomes

saturated and can no longer reach Rs (80kΩ-400kΩ), hence the total impedance of 1S1Rs remains positive. The OTS current must decrease to a minimum holding level to trigger the switch-off, as shown in **Figs. 5a**.

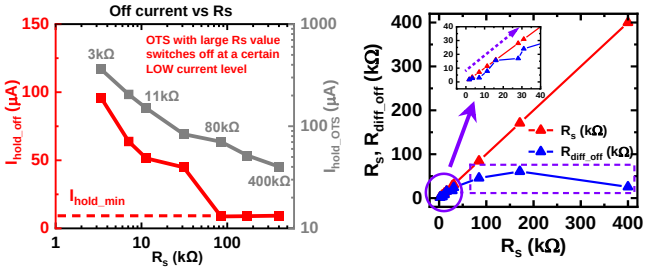

Fig.5 (a) I_{hold_OTS} and I_{hold_off} vs Rs for OTS-only. OTS switches OFF at a common I_{hold_min} when 80kΩ ≤Rs≤400kΩ. (b) R_{diff_off} is plotted vs Rs. For smaller Rs (inset), OTS switches off when $Rs+R_{diff\_OTS}$ =0. For larger Rs, the maximum R_{diff_OTS} is less than 80 kΩ, OTS switches OFF when it reaches the minimum I_{hold}.

As shown in **Fig. 6a**, the inverse of the slopes of normalized I-V curves in the NDR region has a peak in the middle of the NL-ON region, where the R_{diff_OTS} reaches the maximum value, for both the OTS-only and the 1S1R operations. Hence the shrinking speed of the defect cluster accelerates at the beginning of NL-ON. After the peak, the speed starts to reduce as the current decreases further and eventually the clusters rupture at the minimum current for Rs≥80kΩ.

It is observed in **Fig.6b** that both I_{OTS} and V_{OTS} show two regions in the NL-ON range, (I_{hold_OTS} - I_{hold_off}) and (V_{hold_off} -V_{hold_OTS}), and its Rs dependence. One is from ~2kΩ to 30 kΩ, and this is the region that $|R_{diff\_OTS}|$ can become large enough to reach the smaller Rs value, in which both I_{hold_off} and V_{hold_off} change slightly; and the other one is from 80kΩ to 400kΩ where the OTS switch off at the same I_{hold_min} level and at a much larger V_{hold_off}. Hence the full OTS switch-off characteristics and two different switch-off mechanisms are revealed.

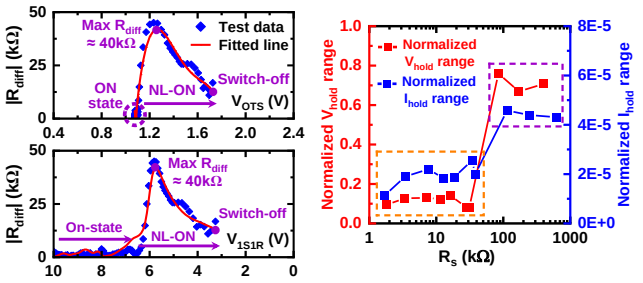

Fig.6 (a) I_{hold_OTS} and I_{hold_off} vs Rs for OTS-only. OTS switches OFF at a common I_{hold_min} when 80kΩ ≤Rs≤400kΩ. (b) R_{diff_off} is plotted vs Rs. For smaller Rs (inset), OTS switches off when $Rs+R_{diff\_OTS}$ =0. For larger Rs, the maximum R_{diff_OTS} is less than 80 kΩ, OTS switches OFF when it reaches the minimum I_{hold}.

When the OTS current reduces, the defect clusters start to shrink, and the defect number in the clusters reduces, so that $|R_{diff\_OTS}|$ increases and V_{OTS} increases. When $|R_{diff\_OTS}|$ reaches the Rs (≤30kΩ), the total impedance of 1S1Rs becomes 0 and the OTS is out of equilibrium and switches OFF at V_{hold_off}. For larger Rs (≥80kΩ), the maximum $|R_{diff\_OTS}|$ value can no longer reach Rs, the OTS is forced to operate at NL-ON state in a low current regime, where I_{OTS} keeps decreasing until it is below the minimum OTS holding current, then the conductive cluster is broken and the OTS switches OFF [14]. Hence the I-V trajectory in the NL-ON is determined by defect clusters.

4. Conclusions

Experimental evidence in this work shed new insights into the full switching-off process of GeAsTe OTS and its dependence on the series resistance value. When the Rs is small, the OTS switches off when the total differential resistance reaches zero. When the Rs value is large, the OTS switches off at a constant minimum OTS holding current level. The changes in $|R_{diff\_OTS}|$ during the switching-off process can be attributed to the defect cluster shrinking kinetics in the OTS and can be therefore measured and characterized. The resulted non-linear ON region and the dependence on the resistance level in the memory element have a significant impact on the parameters and simulation of 1S1R operation.

Acknowledgments

EPSRC UK grant EP/S000259/1 & EP/Y008235/1. The authors would like to thank colleagues at IMEC, Belgium, for test samples and fruitful discussions.

References

[1] G. Burr, et al, J Vac. Sci. & Tech. B, 2014. [2]. J. T. Zhou, et al, IEEE TED, 2014. [3]. H. Cheng, et al, IEDM, 2018. [4]. D. Robayo, et al, IMW, 2019. [5]. S. Jia, et al, Nat Commun, 2020. [6]. Y. Koo, et al, VLSI, 2016. [7]. B. Govoreanu, et al, VLSI 2017. [8]. F. Hatem, et al, Int. Elct. Dev. Meet, 2019. [9]. D. Eaton, et al, J. American Ceramic Society, 1964. [10]. N. Mott, Philosophical Magazine, 1971. [11]. D. Adler, J. Appl. Phys., 1980. 17. [12]. V. G. Karpov, Appl. Phys. Lett., 2007. [13]. S. Kabuyanagi, et al, VLSI 2020. [14]. R. Degraeve, IRPS, 2021. [15]. S. Clima, et al, Physica Status Solidi-Rapid Research Lett., 2020. [16]. P. Noe, et al, Sci Adv, 2020. [17]. J. M. Lopezet al, IMW2021. [18]. C. Wu, et al, VLSI, 2021. [19]. Pryor et al, J. Non-Crystalline Solids, 1972. [20]. A. J. Hughes, et al, J. Non-Crystalline Solids, 1975. [21]. Y. Yu, et al, ACS Appl. Electr. Mat., 2020. [22]. S. Lavizzariet et al, IEEE TED, 2010. [23]. D. Garbin, et al, IEDM, 2019. [24]. W. Devulder, et al, Thin Solid Films, 2022.